

# CHEMPHYSCHEM

## Supporting Information

© Copyright Wiley-VCH Verlag GmbH & Co. KGaA, 69451 Weinheim, 2007

**Supporting information for****Forward and backward pericyclic photochemical reactions have intermediates in common, yet cyclobutenes break the rules**

Werner Fuß <sup>a)\*</sup>, Wolfram E. Schmid <sup>a)</sup>, Sergei A. Trushin <sup>a)</sup>, Paul S. Billone <sup>b)</sup>, William J. Leigh <sup>b)</sup>

<sup>a)</sup> Max-Planck-Institut für Quantenoptik, D-85741 Garching, Germany

<sup>b)</sup> Dept. of Chemistry, McMaster University, 1280 Main Street West, Hamilton, ON L8S 4M1,  
Canada

Fax: +49-89-32905-200, e-mail: w.fuss@mpq.mpg.de

*Methods*

Bicyclo[3.2.0]hept-6-ene and bicyclo[4.2.0]oct-7-ene were prepared by photolysis of a 0.05 M solution (in ca 85 mL portions) of cyclohepta-1,3-diene and 1,3-cycloocta-1,3-diene, respectively (Sigma-Aldrich) in n-pentane (BDH Omnisolv) with a low pressure mercury lamp in a water-cooled immersion well apparatus fitted with a Vycor inner sleeve, as previously described <sup>[1]</sup>. The compounds were isolated by semi-preparative gas chromatography (20% TCEP on 80/100 Chromosorb PNAW; 3 m x 4 mm glass; Chromatographic Specialties, Inc.) after concentration of the combined solutions from several runs by slow distillation and bulb-to-bulb distillation of the residue under vacuum. Capillary GC analysis (100 m x 0.25 mm Petrocol-DH; Supelco, Inc.) indicated the resulting material to be of >98.5% purity, and contained <0.1% of the diene.

The pump pulses (196 nm, 150 fs,  $10^9$  W cm<sup>-2</sup>) were generated from a Ti-sapphire laser system combined with an optical parametric generator and various nonlinear frequency conversions. The fundamental of the laser (805 nm, 45 fs,  $1-3 \times 10^{13}$  W cm<sup>-2</sup>, polarization 55° versus the pump) served for probing by ionization after a variable delay. Both lasers are focused (focal length 1 and 0.7 m for pump and probe, focal diameters  $\leq 0.1$  mm) into the ion source of a time-of-flight mass spectrometer; the UV laser excites about 0.1% of the molecules per pulse, and due to the long free path lengths, the molecules are easily exchanged in the time (1 ms) between the pulses. Using pressures of  $10^{-7}$  –  $10^{-4}$  mbar at 20 °C, the yields of the parent M<sup>+</sup> and two fragment ions (M<sup>+</sup>-15 for both compounds, masses 66 and 68 u for BCH6 and mass 79 and 41 u for BCO7) were determined in a time-of-flight mass spectrometer. These signals were simulated by sums of exponentials, with convolution of the pump and probe pulses where necessary (i.e., at short

times), in order to determine time constants  $t_i$ . The  $t_i$  represent lifetimes of observation windows  $L_j$ , i.e., locations on the potential surfaces, and the probabilities (contained in the preexponential factors, also listed in the tables) to produce an ion of mass  $m$  from location  $L_j$  of the excited molecules. The  ${}^mS_j$ , as functions of  $m$ , in principle represent mass spectra (fragmentation patterns) of the different  $L_j$ ; however, the relative magnitudes of the  ${}^mS_j$  for different  $m$  are not certain, because typically only one  $m$  was investigated in each run. Relative energies of the locations  $L_j$  can be estimated (1) from the order of ionization on varying the probe intensity and (2) from the fragmentation patterns (see below). Details of the setup and evaluation are given elsewhere <sup>[2]</sup>.

## Results

The photoionization mass spectrum of BCH6 (Fig. S1a), measured at a delay of 100 fs of the 805-nm probe pulse shows three strong peaks: the parent (94 u) and two fragment (79 and 66 u) ion signals. All three were also studied with time resolution (Fig. S2). The mass spectrum of CHD (Fig. S1b <sup>[3]</sup>) shows only a minor difference (to be discussed below after Table S4). The mass spectrum of BCO7, measured at a delay of 30 fs (Fig. S1c), exhibits the parent (108 u) and several fragment ions. For time resolution, we chose the signals at 108, 93, 79 and 41 u. The mass spectrum of the isomeric COD <sup>[3]</sup> is not shown in Fig. S1, because is not distinguishable from that of its isomer BCO7.

The time-dependent signals for BCH6 and BCO7 are shown in Figs. S2 and S3, respectively, together with the Xe<sup>+</sup> signal. The latter is obtained from added Xe by ionization by 1 pump photon + 4 probe photons. Its maximum indicates the time zero. Its shape is the correlation function of the pump pulse with the fourth power of the probe pulse. Since the latter is much shorter than the former, the shape of this function is practically independent of the order  $n$  of ionization by the probe, if  $n \geq 3$ . This is the case for the investigated molecules only for the locations after some relaxation, so that for them the Xe signal can be taken as the instrumental function, with which the exponentially decaying populations must be convoluted to simulate the signals. The half-width of the pump pulse (150 fs) was also evaluated from the Xe curve; the duration of the probe pulse (45 fs) was determined by a commercial autocorrelator. From the shapes of pump and probe pulses we calculated the instrumental functions for  $n < 3$ . For the Franck-Condon region ( $L_1$ ) of BCH6 we used  $n = 2$ . This is based on the  $L_1$  energy, which is equal to that of the pump photon (6.33 eV, 196 nm), and the ionization energy (9.0 eV for BCO7 <sup>[4]</sup>, probably similar for BCH6) and the energy of the probe photon (1.53 eV, 810 nm). For

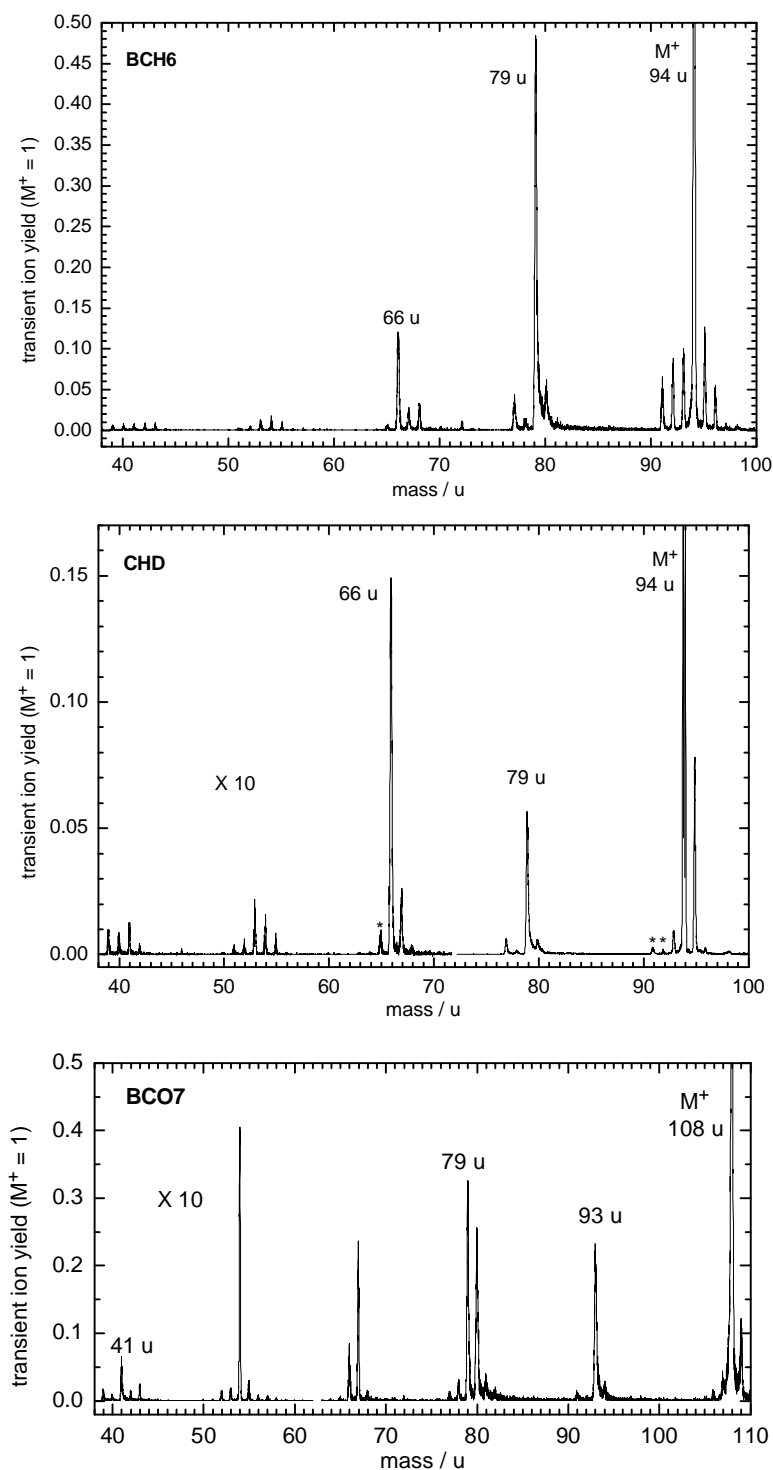


*Fig. S1.* Photoionization mass spectra of BCH6, CHD and BCO7. The first two were measured with the probe delayed by 100 fs after the pump, that of BCO7 with a delay of 30 fs. Note that the lower-mass (<72 u) signals in the spectrum of CHD have been magnified; peaks marked with an asterisk are due to an impurity<sup>[3,6]</sup>. A magnified section is also shown for the lower mass range of BCO7.

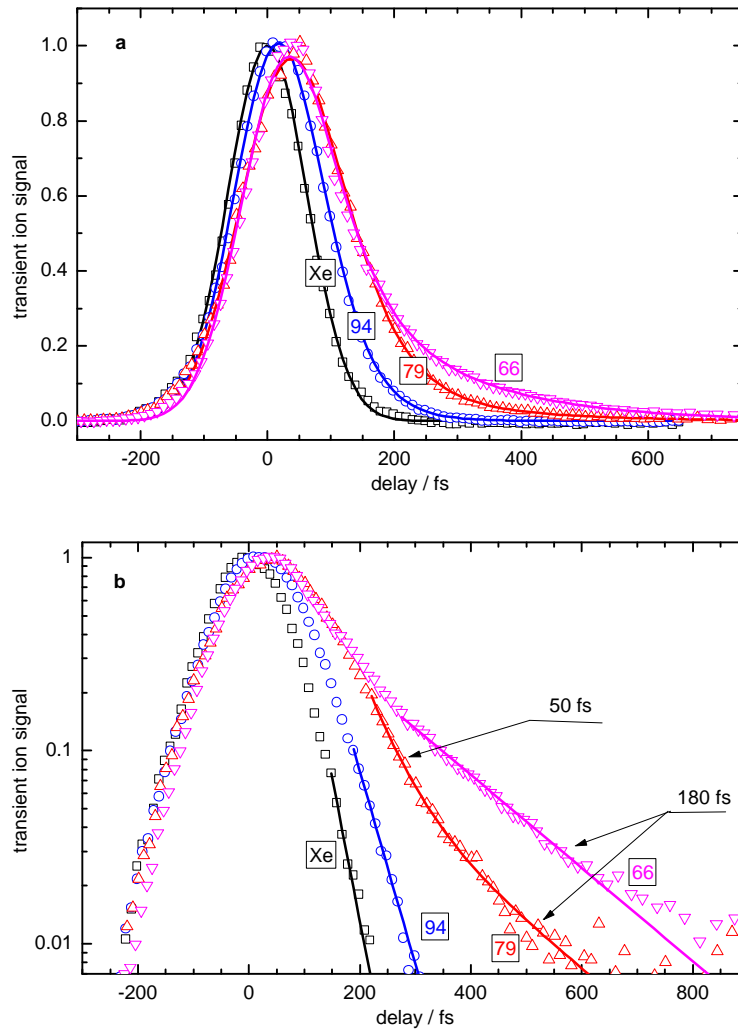


*Fig S2.* Time-dependent signals from BCH6 at the indicated masses in linear (a) and logarithmic (b) scales. The Xe<sup>+</sup> signal (instrumental function) is shown for comparison.

BCO7, however, the parent ion signal is clearly broader than any instrumental function with  $n \geq 2$  (compare the left wing of the 108-u signal with the Xe data in Fig. S3). Therefore we varied  $n$  as a parameter in the simulation of the parent ion and found  $n = 0.45$ . This means that there is a good intermediate resonance for two-photon ionization by the probe laser from the Franck-Condon region of BCO7 and that both absorption steps are saturated to a large degree. Note that there are no such problems with the fragment signals (Fig. S3); they mainly come from lower, relaxed locations, that have higher ionization energies and seem not to meet comparable resonances.

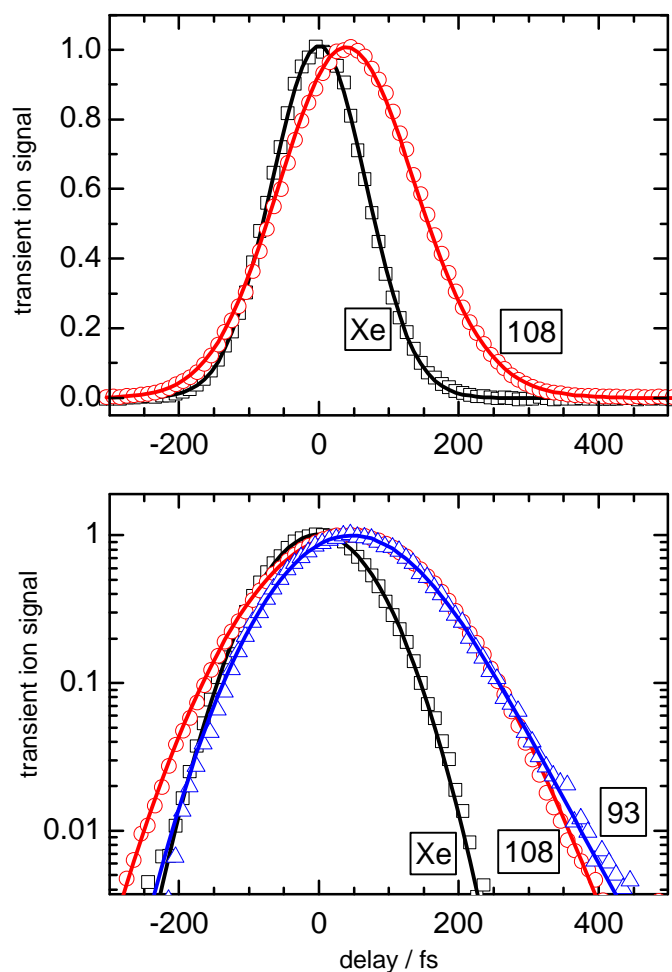


*Fig. S3.* Time-dependent signals from BCO7 at the parent (108 u) and a fragment (93 u) mass in linear (a) and logarithmic (b) scales. The signal at mass 41 u has been omitted to avoid too much overlap of the data. In the linear scale, the fragment ions are not distinguishable from the parent ion. The Xe<sup>+</sup> signal (instrumental function) is shown for comparison.

The three BCH6 signals are shown in Fig. S2. The logarithmic part (Fig. S2b) also shows straight lines in the tails, representing exponential decays at times when convolution with the instrumental function can already be neglected. Although there is no decay in Xe, the Xe<sup>+</sup> signal is also fitted to such a line, its slope corresponding to 30 fs. Such an exponential tail cannot be distinguished from a Gaussian due to the relatively low signal-to-noise ratio in this region. This means that the available pulses permit determination of time constants  $t_i(\text{CB})$  only when (a)  $t_i(\text{CB}) \geq 30$  fs and (b) the signals are larger than  $\approx 0.5\%$  of the maximum. The latter restriction prevented detection of a  $t_4$  process in BCO7, affording the conclusion that the process is much less significant in this molecule than in BCH6; compare Figs. S2 and S3). It also prevented detection of reactions occurring after return to the ground state. (Reactions in the hot ground state, detected with the

two *cis,cis*-dienes after excitation at longer wavelength, which provides better signal-to-noise ratio, were identified by comparing their time constants  $t_5(\text{ccD})$  to estimates of the rate constants for ring closure of the strained *cis,trans*-isomers. This assignment also allowed identification of the preceding step – departure from  $L_3$  within  $t_3$  – as due to *cis*→*trans* isomerization, and thus the assignment of  $L_3$  to  $\text{ct}^*$  [3].)

With BCO7 (Fig. S3) the 93-u and 79-u signals practically coincide. The fragment signals including that at mass 41 u differ from the parent ion by showing a part with time constant ( $t_3 =$ ) 53 fs, which is visible at long delay times. (The  $\text{M}^+$  signal does not contain  $t_3$ .) To avoid congestion, we show in Fig. S3 only the signals at 108 and 93 u in the logarithmic part and 108 u in the linear part. Due to the less pronounced separation of the different decay phases in BCO7 than in BCH6, much more signal averaging was carried out and more fragment signals were investigated. The study of the very weak fragment signal at 41 u had the same motivation: Because fragmentation increases on the way down the potential surfaces, such a small mass should show the later observation windows more clearly than heavier masses; this was indeed the case. The comparison of all the signals allows us to establish the time constants in Table 1 (and Table S2 below).

The time constants obtained from the fit-line slopes of Figs. S2b and S3b were used as starting values for a full simulation of the signals (curves in Figs. S2a and S3a); this simulation did practically not change their values, however. The functions used for the simulation are based on rate equations: They are sums of exponentials with time constants  $t_i$  and coefficients containing ratios of rate constants and  $^m\mathbf{s}_i$  (multiplied by branching factors where appropriate, see below), convoluted with the instrumental function. The  $t_i$  are depopulation times of locations  $L_i$  (observation windows) on the potential surfaces (or appearance times of  $L_{i+1}$ ), and the  $^m\mathbf{s}_i$  are the corresponding probabilities to produce an ion of mass  $m$  from  $L_i$ . The form without branching ratios results from rate equations with a purely consecutive flow of population ( $L_1 \rightarrow L_2 \rightarrow L_3 \rightarrow L_4 \rightarrow \dots$ ). However, for BCH6 the data fit better (see below) to a scheme with branching in  $L_2$ ; that is,  $L_3$  and  $L_4$  are both populated simultaneously from  $L_2$ , and (separate parts of) the  $S_0$  surface is then reached from  $L_3$  and  $L_4$ . We assumed a ratio of branching factors of 0.5 : 0.5, estimated from the ratio of signals (see main text). For BCO7, the corresponding branching ratio seems to be smaller, disfavoring  $p^*$ ; a purely consecutive analysis was therefore applied for this molecule.

Table S1 compiles for BCH6 the  $t_i$  and  $^m\mathbf{s}_i$ , evaluated for both, the purely consecutive and the branched cases. The time constants are not distinguishable for the two cases. The table also

shows a column indicating " $t_{0/1}(\text{BCH6}) = 0$  fs". This means that there is either a time constant  $t_1$  below time resolution, i.e.,  $<30$  fs, or (and) there is a contribution from nonresonant two-color ionization during the pump-probe overlapping time; the latter process is sometimes observed (e.g., in <sup>[5]</sup>) and can then be simulated by an apparent time constant (" $t_0$ ") of 0 fs. Whereas the numbers in the  $t_{0/1}$  column result from this type of simulation, we assume that there also exists a real (nonvanishing) time constant  $t_1(\text{BCH6}) < 30$  fs, and Fig. 2 in the main text has been drawn accordingly. This assumption is supported by the fact that such a  $t_1$  has been observed in the homologous BCH6 and in many other olefins and polyenes (see, e.g., <sup>[3, 6]</sup>).

Table S2 lists the corresponding data for BCO7. In contrast to BCH6, the first time constant  $t_1$  (= 30 fs) was directly measurable. All data for this molecule are consistent with purely consecutive processes, and the data of the table are based on such a model. We made an effort also to detect signals from  $L_4$  (with time constant  $t_4$ , expected in the range  $>t_3(\text{BCO7})$  but  $<t_4(\text{COD})$ , hence  $50$  fs  $< t_4 < 118$  fs), analogous to that of BCH6 and the dienes. However, the signals in this time range were  $<0.5\%$  of the signal maxima, so that they should not be evaluated in this range. For instance,  ${}^{93}\mathbf{s}_4 < 0.005$ . Comparing with  ${}^{93}\mathbf{s}_3 = 0.17$  and taking the ratio of ionization probabilities from  $L_4$  and  $L_3$  to be 1:10 as in COD <sup>[3]</sup> implies that the branching ratio to  $L_4$  and  $L_3$  is  $<0.25:0.75$ . (For BCH6 it is near 0.5:0.5, see above.)

*Table S1.* Time constants  $t_i(\text{BCH6})$  (lifetimes of locations  $L_i$ ) and probabilities  ${}^m\mathbf{s}_i$  to produce an ion of mass  $m$  from location  $L_i$  of excited BCH6. The  ${}^m\mathbf{s}_i$  differ as indicated for the purely consecutive and the branched (branching ratio 1:1) models, whereas the lifetimes are the same.

| $i$                                 | 0/1                | 2          | 3          | 4            |
|-------------------------------------|--------------------|------------|------------|--------------|
| $t_i/\text{fs}$ <sup>a)</sup>       | 0 / $<30$          | $44 \pm 4$ | $50 \pm 4$ | $180 \pm 20$ |
| ${}^{94}\mathbf{s}_i$               | 0.45 <sup>b)</sup> | 1.0        | 0          | 0            |
| ${}^{79}\mathbf{s}_i$ (consecutive) | 0.21 <sup>b)</sup> | 1.0        | 0.30       | 0.03         |
| ${}^{79}\mathbf{s}_i$ (branch ct*)  |                    |            | 0.30       | –            |
| ${}^{79}\mathbf{s}_i$ (branch p*)   |                    |            | –          | 0.03         |
| ${}^{66}\mathbf{s}_i$ (consecutive) | 0.21 <sup>b)</sup> | 1.0        | 0.32       | 0.11         |
| ${}^{66}\mathbf{s}_i$ (branch ct*)  |                    |            | 0.32       | –            |
| ${}^{66}\mathbf{s}_i$ (branch p*)   |                    |            | –          | 0.11         |

<sup>a)</sup> Error limits are standard deviations of values obtained in  $\geq 10$  runs.

<sup>b)</sup> The instrumental function is multiplied by these numbers to get the  $L_0$  ( $t_0 = 0$ ) contribution to the signals. Although we assume that there is a contribution with a time constant  $t_1 > 0$ , the corresponding  ${}^m\mathbf{s}_1$  could not be unambiguously evaluated.

Table S2. Time constants  $t_i(\text{BCO7})$  (lifetimes of locations  $L_i$ ) and probabilities  ${}^m\mathbf{S}_i$  to produce an ion of mass  $m$  from location  $L_i$  of excited BCO7. A purely consecutive sequence of processes was assumed, because any branching (implying an additional time constant  $t_4$ ) could not be established.

| $i$                           | 1                | 2                | 3          |
|-------------------------------|------------------|------------------|------------|
| $t_i/\text{fs}$ <sup>a)</sup> | 30 <sup>b)</sup> | 30 <sup>b)</sup> | $53 \pm 3$ |
| ${}^{108}\mathbf{S}_i$        | 1.0              | 0.8              | $<0.005$   |
| ${}^{93}\mathbf{S}_i$         | 0.8              | 1.0              | 0.17       |
| ${}^{41}\mathbf{S}_i$         | 0.385            | 1.0              | 0.1        |

a) Error limits are standard deviations of values obtained in  $\geq 10$  runs.

b)  $t_1 + t_2 = 60 \pm 6$  fs. The error limits for the individual constants could not be determined.

## Assignment

It is said in the main text that the observation windows  $L_i$  not only differ in their ionization probabilities ( $\sum_m {}^m\mathbf{S}_i$ ) but also in their fragmentation patterns ( ${}^m\mathbf{S}_i$  for each  $i$ ) and orders of ionization  $n$ . In fact, the ionization probability drops to below the detection limit, when the cyclobutenes return to the (reactant or product) ground states; the order of ionization is expected to change from  $n = 2$  in the Franck-Condon region (see above) to  $n = 6$  in  $S_0$ , corresponding to the ionization energies (9.0 eV for BCO7 <sup>[4]</sup>, probably similar for BCH6). (In the dienes, due to the better signal-to noise ratio, the ground-state signals due to ctD were also detected <sup>[3]</sup>.) The columns ( ${}^m\mathbf{S}_i$  for given  $i$ ) of Tables S1 and S2 reflect the fragmentation patterns. However, they are not identical to the real mass spectra, because the signals at each mass  $m$  (each horizontal line in the tables) are normalized to the strongest peak. But one can recognize, how fragmentation changes from  $L_i$  to  $L_{i+1}$  by comparing the columns.

For example, the signal ratios for  $M^+$  and  $M^+-15$  differ by only a factor of  $<2$  between  $L_1$  and  $L_2$  in BCO7 (in BCH6,  $L_1$  could not be evaluated), but by a factor of  $>30$  between  $L_2$  and  $L_3$  for BCO7 and even more for BCH6. This means that the parent ion initially produced from  $L_3$  and  $L_4$  has much more excess energy than if produced from  $L_1$  or  $L_2$ , so that it fragments extensively after it is generated by ionization. The excess energy can already be present in (neutral)  $L_3$  and  $L_4$  due to a lower electronic energy ("vertical displacement"); it can also be caused by a horizontal displacement (because where the neutral potentials drop along a reaction coordinate, the potentials of the ions usually rise, so that higher-energy states are reached on ionization) and/or to special reasons such as selection rules. In the main text, we invoke the selection rule that from

the two-electron excited 2A state, ionization produces an electronically excited ion. This mechanism alters the ionic excess energy suddenly, whereas the former two mechanisms will give rise to smoother changes. Therefore we attribute the sudden change on leaving  $L_2$  in these molecules (as in many other pericyclic and some other reactions<sup>[3,6]</sup>) to a relaxation from a one-electron excited (1B) to a two-electron excited (2A) state. Very recently this assignment was independently confirmed by detection of the transient photoelectron spectra (including the time constants) from the 1B and 2A states on electrocyclic ring opening of 1,3-cyclohexadiene<sup>[7]</sup>.

The fragmentation difference between  $L_3$  and  $L_4$  of BCH6 (in BCO7,  $L_4$  signals were below the detection limit) can be judged from the ratios  $^{79}\mathbf{S}_i/^{66}\mathbf{S}_i$ , which is 0.94 for  $i = 3$  and 0.27 for  $i = 4$ . This change (by a factor of 3.5) is small, similar as that between  $L_1$  and  $L_2$  (factor of  $<2$ ) for which we concluded above that they are on the same electronic surface (1B), with  $L_2$  representing a lower location. We can hence also assume that  $L_3$  and  $L_4$  are on one surface (2A), with  $L_4$  a bit lower than  $L_3$ . (With the dienes, also signals from the ground states could be detected<sup>[3]</sup>. Their mass spectra showed drastically more fragmentation than from the preceding levels  $L_3$ .)

To determine the order  $n_i$  of ionization of the location  $L_i$  from the dependence on probe intensity, it would be desirable to measure the sum of the ion yields with different masses. But this method is not directly applicable, because the different masses have been studied in separate runs and their intensities normalized to the strongest signal (which originates from  $L_2$  in BCH6, see Table S2). For comparing the relative order of ionization, we took a strong fragment instead of any sum. (Weak fragment signals may be more strongly affected by the increase of the degree of fragmentation at higher laser intensities.) For BCH6 we chose mass 79. The data are given in Table S3.

Table S3. Signal intensities  $^{79}\mathbf{S}_i$  (relative to  $^{79}\mathbf{S}_2$ ) for BCH6 with different probe laser intensities. (The data of Table S1 were obtained from several runs with probe laser energies near 10 TW  $\text{cm}^{-2}$ .)

| $L_i$   | 1   | 2                 | 3    | 4     |
|---|-----|-------------------|------|-------|
| $^{79}\mathbf{S}_i$ (10 TW $\text{cm}^{-2}$ ) | –a) | 1.0 <sup>b)</sup> | 0.28 | 0.024 |
| $^{79}\mathbf{S}_i$ (20 TW $\text{cm}^{-2}$ ) | –a) | 1.0 <sup>b)</sup> | 0.68 | 0.047 |

a) The  $^m\mathbf{S}_i$  corresponding to an assumed time constant  $\tau_1 > 0$ , were not be evaluated. See also footnote<sup>b)</sup> of Table S1.

b) Normalized.

Obviously on raising the laser energy by a factor of 2, the signals from  $L_3$  and  $L_4$  increase both by practically the same factor of  $\approx 2$ . This means that  $n_3 = n_4 = n_2 + 1$  or  $n_3 = n_4 = 3$ , if  $n_2 = 2$  is

inferred from the ionization energy. ( $n_2 = 2$  is also consistent with the simulation of the  $M^+$  signals, which come only from  $L_1$  and  $L_2$ .) The equality  $n_3 = n_4$  means that  $L_3$  and  $L_4$  have approximately the same ionization energy and probably also the same energy, which is lower (by a substantial fraction of the energy of one photon, 1.55 eV) than that of  $L_2$ . The method was not applicable to BCO7, where  $L_4$  was not detected. With the dienes, also the locations  $L_1$  and  $L_2$  could be compared ( $n_1 = n_2$ ), and in addition two ground-state locations ( $n_5 = n_6 \approx n_{3(4)} + 1$ )<sup>[3]</sup>. We should, however, mention that the degree of fragmentation is in general a more sensitive function of small energy differences than the order of ionization.

As in the dienes<sup>[3]</sup> and other cases,  $t_1(\text{CB})$  will represent the time for population flowing out of the Franck-Condon region of the pumped 1B state; accordingly, fragmentation is lowest in this window  $L_1$  (compare, for example for BCO7, the ratios of  $mS_1$  with those of  $mS_2$  or  $mS_3$  in the columns of Table S3, etc.). The initial relaxation direction is given by the Franck-Condon active coordinate (which can be defined in this way). As argued above, transition to the (lower) 2A surface takes place during  $t_2(\text{CB})$ .  $L_3$  and  $L_4$  will then be locations on this surface, from where population flows within  $t_3$  and  $t_4$  to the ground state.

Although only an upper limit of population of any  $L_4$  location can be given for BCO7 (see above), we assume that it is present in analogy with BCH6 and is populated in competition with  $L_3$ . The process is assumed to branch within  $t_2$ . Although there will be two rate constants for depopulation of  $L_2$ , ( $k_{2a}$  and  $k_{2b}$ , whose ratio is the branching ratio), there will be only one observable time constant  $t_2 = (k_{2a} + k_{2b})^{-1}$ ;  $L_3$  and  $L_4$  appear within the same time as  $L_2$  disappears. For BCH6 and the dienes, the assumption of branching in  $L_2$  is justified by investigating the properties of  $L_3$  and  $L_4$ . This was done in detail for the dynamics of two dienes, *cis,cis*-cyclohepta-1,3-diene (CHD, whose ring closure results in BCH6) and *cis,cis*-cycloocta-1,3-diene (COD, whose ring closure results in BCO7)<sup>[3]</sup>. We compared their relative energies, estimated from the orders of ionization and the fragmentation patterns, and demonstrated that on comparing these two homologous molecules the relative  $L_3/L_4$  populations vary by the same factor (of 9) as the known quantum yields for the two competing channels ring closure and *cis-trans*-isomerization. In this context it is interesting – and probably not unexpected – that the  $L_3/L_4$  population ratio is also smaller for the heavier cyclobutene (BCO7 versus BCH6).

The statement that  $L_3$  and  $L_4$  are in common for forward and backward reactions is inferred from a comparison of the isomeric pairs CHD/BCH6 and COD/BCO7. The evidence is based on the following observations:

1. The equality of time constants  $t_3(\text{ccD}) = t_3(\text{CB})$  not only for the pair CHD/BCH6 but also for COD/BCO7. Such an equality for *two* pairs of isomers can hardly be accidental.
2. The expected shortening of  $t_4(\text{CHD})$  to  $t_4(\text{BCH6})$  due to the higher excess energy on starting from BCH6. A shortening is expected, because the long  $t_4(\text{CHD})$  implies a (small) activation energy. By contrast, the shorter  $t_3$  implies a (nearly) barrierless process, so that no shortening by excess energy is expected for this channel.
3. On going from BCH6 to BCO7, the  $L_4/L_3$  signal ratio drops (by a factor  $>3$ ) to below the detection limit. This is similar to the decrease of this ratio (by a factor  $\approx 9$ ) on going from CHD to COD.
4. The order of ionization is the same for  $L_3$  and  $L_4$ , whether coming from the diene or the cyclobutene (BCH6) side.

Although each individual argument is not a compelling proof, the four together are a better support of the idea of common intermediate states. The model is made even more credible by its successful explanation (and lack of alternative explanations) of the different specificities of forward and backward reactions and other observations (see main text), and by the fact that it is only a slight modification of the generally accepted scheme – involving a pericyclic minimum – for pericyclic photochemical reactions.

The fragmentation patterns are slightly different for  $L_3$  (and  $L_4$ ) for the forward and backward reaction. One expects that fragmentation from a common level ( $L_3$  or  $L_4$ ) is more extensive, if one starts with higher excess energy, i.e., from the cyclobutene side. This is indeed the case for  $L_3$  of the COD/BCO7 pair and for  $L_4$  of the CHD/BCH6 pair. But surprisingly for  $L_3$  the ratio is smaller from the CHD side than from the BCH7 side, as shown in Table S4, which lists the ratios of the signals with masses 79 u and 66 u.

*Table S4.* Ratio of signals at 79 u to those at 66 u from different locations  $L_i$  on the potential surface, starting from BCH6 and CHD, respectively. These values were retrieved by renormalization of the values in Table S1 by the help of the mass spectra in Fig. S1.

|      | $L_1$ | $L_2$ | $L_3$ | $L_4$ |
|------|-------|-------|-------|-------|
| BCH6 | 4.8/1 | 3.7/1 | 4.7/1 | 1.2/1 |
| CHD  |       |       | 2.6/1 | 2.6/1 |

At first sight, this observation seems not consistent with the idea that  $L_3$  is a common intermediate for the CHD/BCH6 pair (in spite of the evidence above and although also fragmentation indicates that  $L_4$  is common for this pair and  $L_3$  is common for COD and BCO7).

A possible reason for the slight difference of the fragmentation patterns is revealed by a closer comparison of the mass spectra of BCH6 and CHD, measured at a delay of 100 fs after the pump pulse (Fig. S1). Fragmentation (the ratio of the 79-u and 66-u signals to the parent) of the bicyclic compound is indeed 10 times higher than of the diene; because the 79-u/66-u ratio is unchanged ( $\approx 4$ ), the energy to form these two fragments is obviously very similar, so that already minor differences in the reaction path may change this ratio. The mass spectrum of BCH6 also contains a (weak) signal at 68 u, which is absent in CHD. Here it should be remembered that in contrast to the diene the bicyclic compound undergoes an additional photoreaction with quantum yield 0.14 (as compared with that for ring opening of 0.12<sup>[1]</sup>), namely ring cleavage to cyclopentene (mass 68 u) + acetylene. The additional peak is probably due to this additional channel; it will come from a location  $L_{cl}$  on the cleavage path, still on the 2A surface. Therefore we did time-resolved measurements also with the fragment of mass 68 u. This signal was found to exhibit a time constant of  $t_{cl}(BCH6) = 50$  fs, in addition to the preceding  $t_2(BCH6)$  and  $\tau_{0/1}$ . That is, accidentally  $t_{cl}(BCH6) = t_3(BCH6)$ . If the mass spectrum of  $L_{cl}$  contains also a strong peak at 79 u (note that cleavage is only completed on the ground state surface), the higher 79-u/66-u ratio in the 50-fs window (column  $L_3$  in Table S3) is rationalized.

## References

- [1] K. B. Clark, W. J. Leigh, *J. Am. Chem. Soc.* **1987**, *109*, 6086-6092.
- [2] W. Fuß, W. E. Schmid, S. A. Trushin, *J. Chem. Phys.* **2000**, *112*, 8347-8362; T. Yatsushashi, S. A. Trushin, W. Fuß, W. Rettig, W. E. Schmid, S. Zilberg, *Chem. Phys.* **2004**, *296*, 1-12; S. A. Trushin, T. Yatsushashi, W. Fuß, W. E. Schmid, *Chem. Phys. Lett.* **2003**, *376*, 282-291.
- [3] W. Fuß, S. Panja, W. E. Schmid, S. A. Trushin, *Mol. Phys.* **2006**, *104*, 1133-1143.
- [4] W. J. Leigh, K. Zheng, N. Nguyen, N. H. Werstiuk, J. Ma, *J. Am. Chem. Soc.* **1991**, *113*, 4993-4999.
- [5] W. Fuß, C. Kosmidis, W. E. Schmid, S. A. Trushin, *Chem. Phys. Lett.* **2004**, *385*, 423-430.
- [6] W. Fuß, S. Lochbrunner, A. M. Müller, T. Schikarski, W. E. Schmid, S. A. Trushin, *Chem. Phys.* **1998**, *232*, 161-174.
- [7] N. Kuthirummal, F. M. Rudakov, C. L. Evans, P. M. Weber, *J. Chem. Phys.* **2006**, *125*, 133307 1-8.